Phase diagrams and tricritical behavior of a diluted spin-1 transverse Ising model in a random field

E. F. Sarmento* and T. Kaneyoshi
Department of Physics, Nagoya University, 464-01, Nagoya, Japan
(Received 22 June 1992; revised manuscript received 25 March 1993)

Phase diagrams and magnetization curves of a diluted spin-1 transverse Ising model in a random field on honeycomb, square, and simple-cubic lattices, respectively, are investigated by the use of an effective-field theory with correlations. The tricritical point is found in the system, in contrast to the corresponding spin-$\frac{1}{2}$ Ising counterpart. The behavior of the tricritical point is also examined as a function of applied transverse field. The possible reentrant phenomena displayed by the system due to the competition effects that occur for appropriate ranges of the random and transverse fields are investigated.

I. INTRODUCTION

The two-state transverse Ising model,[1] was originally introduced as a valuable model for hydrogen-bounded ferroelectrics[2] such as the KH_2PO_4 type. Since then, it has successfully been used to study a number of problems of phase transitions associated to order-disorder phenomena in several other systems, for example, cooperative Jahn-Teller[3] (such as D_yVO_4 and T_bVO_4) and some real magnetic materials for which the crystal-field ground state is a singlet.[4] The wider applicability of the model has extensively been reviewed in the literature.[5,6] The model is described by a two-state Ising Hamiltonian with a term representing a field transverse to the Ising spins, namely,

$$\mathcal{H}=-\tfrac{1}{2}\sum_{i,j}J_{ij}\sigma_i^z\sigma_j^z-\Omega\sum_i\sigma_i^x , \tag{1}$$

where σ_i^z and σ_i^x are components of a spin-$\frac{1}{2}$ operator at site i, J_{ij} is an exchange interaction, Ω represents a transverse field, and the sums extend over all the points of a lattice.

The thermodynamical properties of the model Hamiltonian Eq. (1) have been exactly obtained only for the one-dimensional lattice.[7–9] In order to study higher dimensional lattices some sort of approximation has to be done, and the problem of finding a solution has generated a number of different approximations schemes.[10–13] However, all these approaches consider only the model Hamiltonian described by Eq. (1) [namely the spin-$\frac{1}{2}$ two-state Ising model (TIM)] and most of them have been restricted to the analysis of particular regimes, either at low- or at high-temperature regions.

On the other hand, the random-field Ising model (RFIM) has received a great amount of interest[14–16] in the last few years because it helps to simulate many interesting but complicated problems. A dilute uniaxial two-sublattice antiferromagnet in a uniform magnetic field fits this model in that random local fields couple linearly to the antiferromagnetic order parameter.[17] It can also be used to describe such processes as the phase separation of a two-component fluid mixture in porous material or gelatin and the solution of hydrogen in metallic alloys.[18] Theoretically, the RFIM has been widely investigated by the use of various techniques, including the mean-field-approximation effective-field theories,[19–21] renormalization calculations,[22,23] and Monte Carlo simulation.[24,25] It has been suggested by Aharony[22] that the second-order region in the phase diagram may be separated from the first-order region by a tricritical point, provided that the symmetric distribution function of the random field has a minimum at zero field. In the Bethe-Peierls approximation,[20] the tricritical point has been found for both $z=3$ and $z=6$, where z is the coordination number, while by using an effective-field theory,[26] Borges and Silva[21] have discussed that the tricritical point does not exist, when z is lower than $z=6$. Moreover, in the two-dimensional case ($z=3$ and $z=4$), the phase diagrams exhibit reentrant phenomena, i.e., two-phase transitions, for the appropriate range of the random field. In consequence of the dramatic effects appearing in the RFIM, there has been an increasing interest in studying other systems in the presence of random fields, such as the Heisenberg model,[27] the transverse Ising model,[28,29] the amorphous Ising ferromagnet,[30] and the Blume-Capel method.[31]

The spin-$\frac{1}{2}$ transverse Ising model in random field[32] has received some attention in recent years.[28,29,33,34] The Hamiltonian of the system is, in addition to Eq. (1),

$$\mathcal{H}=-\tfrac{1}{2}\sum_{i,j}J_{ij}\sigma_i^z\sigma_j^z-\Omega\sum_i\sigma_i^x-\sum_i H_i\sigma_i^z . \tag{2}$$

Here, H_i is a random external field, which is assumed to be randomly distributed according to the bimodal independent probability distribution function $P(H_i)$ as

$$P(H_i)=\tfrac{1}{2}[\delta(H_i-H_0)+\delta(H_i+H_0)] . \tag{3}$$

Depending on the improvements that can be made in the mean-field approximation,[35–37] the phase diagrams show second-order transition lines, tricritical points, and reentrant phase transitions which may be caused by the competition effects that occur for appropriate ranges of the transverse and random fields.

However, the spin-1 transverse Ising model in the presence of a random field is another and more complex and interesting problem. In this paper we investigate the phase diagrams and the magnetization curves of a diluted $S=1$ TIM with random field, on the basis of a generalized Callen relation derived by Sá Barreto, Fittipaldi, and Zeks,[38] and very recently introduced into the spin-1 Ising models.[39–41]

The outline of this work is as follows. In Sec. II, we present the formalism and discuss the effective-field theory with correlations for a diluted spin-1 TIM. In Sec. III we study the phase diagrams and tricritical points for lattices with $z=3$, 4, and 6. The numerical results and discussions are presented in Sec. IV. In Sec. V we discuss the magnetization curves. Finally, in Sec. VI we comment on the results.

II. FORMALISM

We consider a site diluted spin-1 transverse Ising model with a random field, described by the Hamiltonian

$$\mathcal{H}=-\sum_{\langle ij\rangle} J_{ij}S_i^zS_j^z\xi_i\xi_j-\Omega\sum_i S_i^x\xi_i-\sum_i H_iS_i^z\xi_i \ , \quad (4)$$

with nearest-neighbor interaction J_{ij} between spins at sites i and j, S_i^x, $S_i^z=\pm1$, and 0 are spin-1 operators, and ξ_i is a site occupancy number which takes values 1 or 0 depending on whether the site is occupied or not. Ω and H_i are the transverse and random field, respectively, the latter being governed by the distribution probability function given by Eq. (3).

The total Hamiltonian is split into two parts, $\mathcal{H}=\mathcal{H}_n+\mathcal{H}'$. Here $\mathcal{H}_n$ includes all the parts of $\mathcal{H}$ associated with the lattice site n, and $\mathcal{H}'$ represents the rest of Hamiltonian and does not depend on site n for spin operators. Furthermore, we assume that $[\mathcal{H}_n,\mathcal{H}']=[\mathcal{H}_n,\mathcal{H}]\neq0$. By following Sá Barreto, Fittipaldi, and Zeks,[38] after a straightforward calculation we obtain that the average value of a spin operator $\hat{O}_n$ is given by

$$\langle \hat{O}_n\rangle=\left\langle \frac{\mathrm{tr}_{\{n\}}\hat{O}_n e^{-\beta\mathcal{H}_n}}{\mathrm{tr}_{\{n\}}e^{-\beta\mathcal{H}_n}}\right\rangle \ , \quad (5)$$

which can be considered as an approximate generalized Callen[42]-Suzuki[43] identity. Equation (5) is a reasonable approximation and has formed the starting point of many theoretical calculations on transverse Ising system[44–47] and will again be adopted here.

By taking into account Eq. (5), the longitudinal and transverse site magnetizations for our diluted spin-1 transverse Ising system[40] with a random field are given by

$$m_i^z=\langle S_i^z\rangle=\left\langle \frac{\overline{\Theta}_i}{E_i}\frac{2\sinh(\beta E_i)}{1+2\cosh(\beta E_i)}\right\rangle \ , \quad (6)$$

$$m_i^x=\langle S_i^x\rangle=\left\langle \frac{\Omega}{E_i}\frac{2\sinh(\beta E_i)}{1+2\cosh(\beta E_i)}\right\rangle \ , \quad (7)$$

with

$$\overline{\Theta}_i=\sum_j J_{ij}S_j^z\xi_i\xi_j+H_i\xi_i \ , \quad (8)$$

$$E_i=[\Omega^2+\overline{\Theta}_i^2]^{1/2} \ . \quad (9)$$

Here, $\langle\cdots\rangle$ indicates the canonical thermal average and $\beta=1/k_BT$. In the limit $\Omega=0$ with $\xi_i=1$, $m_i^x=0$ and Eq. (6) reproduces the exact identity for the spin-1 Ising model with an external field H_i.[48] Expanding the right-hand side of Eqs. (6) and (7) as a formal series in the spin variables and neglecting correlations of E_i, the standard mean-field-approximation results are recovered.

At this stage, in order to write Eqs. (6) and (7) in a form which is particularly amenable to approximation, let us introduce the differential operator technique[26] as follows:

$$m_i^z=\langle e^{\overline{\Theta}_i\nabla}\rangle F(x+H_i)|_{x=0} \ , \quad (10)$$

$$m_i^x=\langle e^{\overline{\Theta}_i\nabla}\rangle G(x+H_i)|_{x=0} \ , \quad (11)$$

where $\nabla=\partial/\partial x$ is a differential operator and functions $F(x)$ and $G(x)$ are defined by

$$F(x)=\frac{x}{(\Omega^2+x^2)^{1/2}}\frac{2\sinh[\beta(\Omega^2+x^2)^{1/2}]}{1+2\cosh[\beta(\Omega^2+x^2)^{1/2}]} \ , \quad (12)$$

$$G(x)=\frac{\Omega}{(\Omega^2+x^2)^{1/2}}\frac{2\sinh[\beta(\Omega^2+x^2)^{1/2}]}{1+2\cosh[\beta(\Omega^2+x^2)^{1/2}]} \ . \quad (13)$$

If one now uses the Van der Waerder identities for spin-1 operators, the expectation value $\langle\exp(\overline{\Theta}_i\nabla)\rangle$ reduce to

$$\langle e^{\overline{\Theta}_i\nabla}\rangle=\left\langle\prod_j[(S_j^z)^2\cosh(J_{ij}\xi_i\xi_j\nabla)+S_j^z\sinh(J_{ij}\xi_i\xi_j\nabla)+1-(S_j^z)^2]\right\rangle \ . \quad (14)$$

The main purpose of this work is to obtain from the above equations the phase diagrams and the behavior of the longitudinal and transverse magnetizations as functions of the parameters T, Ω, and H. However, it is clear that if we try to treat exactly all the spin-spin correlations which appear through the expansion of the above equations, the problem becomes mathematically untractable. Therefore, some approximations are needed. Here, we restrict ourselves to the simplest approximation in which all high-order spin correlations on the right-hand side of (14) are neglected. It is clear that within this approximation the strict criticality of the system is lost, and its real dimensionality is only partially incorporated through the coordination number of the lattice. Nevertheless, as has been already discussed in several works on spin-1 Ising systems,[49,50] such a framework is quite superior to the ordinary mean-field approximation (MFA), and provides in particular a vanishing critical temperature for one-dimensional systems. This is so because in this type of treatment, relations such as $s_i^2=0$, 1 as well as $s_i^3=s_i$ and $s_i^4=s_i^2$, are taken exactly into account, while in the usual MFA all the self- and multispin correlations are neglected. Based on this approximation, one now decouples the thermal multiple correlation functions occurring on the right-hand side of Eq. (14) according to

$$\langle S_j^z(S_k^z)^2\ldots S_e^z\rangle\cong\langle S_j^z\rangle\langle(S_k^z)^2\rangle\ldots\langle S_e^z\rangle \quad (15)$$

for $j \neq k \neq \cdots \neq l$, thus enabling the average to be taken inside the product sign. For a lattice having only nearest-neighbor interaction $J_{ij}=J$, with coordination number z, Eq. (14) reduces to

$$\langle e^{\bar{\Theta}_i \nabla} \rangle = \prod_{j=1}^{z} [\langle (S_j^z)^2 \rangle \cosh(J\xi_i\xi_j\nabla) + \langle S_j^z \rangle \sinh(J\xi_i\xi_j\nabla) + 1 - \langle (S_j^z)^2 \rangle] . \quad (16)$$

It should be stressed that this equation is for a fixed configuration of occupied sites so the thermal averages are configurationally dependent. As discussed in Refs. 51–53, the statistical accuracy of (15) corresponds to the Zernike approximation[54] of spin-$\frac{1}{2}$ Ising models, when $\Omega=0.0$. In particular, for some special cases, such as surface magnetism and the mixed-spin problem, we can compare the results based on the decoupling approximation with those obtained from the exact calculation and Monte Carlo simulation.[55] These results indicate that the decoupling approximation gives reasonable results.

The next step, as has been previously applied to disordered systems in the literature,[56–58] and references therein, is to carry out the configurational averaging. To make progress, the simplest approximation, as was used for the thermal averaging, of neglecting the correlations between quantities pertaining to different sites will be made. That is $\langle X_i X_j X_k \rangle_r \approx \langle X_i \rangle_r \langle X_j \rangle_r \langle X_k \rangle_r$, from whence it follows that

$$m_z = [pf(q_z, m_z, J_{ij}, \nabla) + 1 - p]^z F(x)|_{x=0} , \quad (17)$$

$$m_x = [pf(q_z, m_z, J_{ij}, \nabla) + 1 - p]^z G(x)|_{x=0} , \quad (18)$$

with

$$f(q_z, m_z, J_{ij}, D) = q_z \cosh(J_{ij}\nabla) + m_i^z \sinh(J_{ij}\nabla) + 1 - q_z , \quad (19)$$

where we have performed the random average $\langle \ldots \rangle_r$, and p is the average site concentration defined by $p = \langle \xi_j \rangle_r$.

At this place, in order to evaluate the longitudinal, as well as, transverse magnetizations, it is necessary to calculate the parameter q_i^z defined by

$$q_i^z = \langle (S_i^z)^2 \rangle . \quad (20)$$

By the use of the relation proposed by Sá Barreto, Fittipaldi, and Zeks[38] and Kaneyoshi, Sarmento, and Fittipaldi,[47] we can also obtain q_i^z in the same way as the evaluation of m_i^z and m_i^x. Thus,

$$q_i^z = \langle e^{\bar{\Theta}_i \nabla} \rangle H(x+H_i)|_{x=0} , \quad (21)$$

where the function $H(x)$ is defined by

$$H(x) = \frac{\Omega^2 + (\Omega^2 + 2x^2)\cosh[\beta(\Omega^2+x^2)^{1/2}]}{(\Omega^2+x^2)\{1+2\cosh[\beta(\Omega^2+x^2)^{1/2}]\}} . \quad (22)$$

For a random-field system, we must perform the random average of H_i according to the independent probability distribution function $P(H_i)$ given by Eq. (3). Then the above quantities m_i^α ($\alpha = z$ or x) and q_i are defined as

$$m_\alpha = \langle m_i^\alpha \rangle_r \quad \text{and} \quad q = \langle q_i \rangle_r ,$$

where $\langle \ldots \rangle_r$ denotes the random-field average. Furthermore, the functions $F(x)$, $G(x)$, and $H(x)$ must be replaced by

$$\begin{aligned} \bar{F}(x) &= \int P(H_i) F(x+H_i) dH_i , \\ \bar{G}(x) &= \int P(H_i) G(x+H_i) dH_i , \\ \bar{H}(x) &= \int P(H_i) H(x+H_i) dH_i . \end{aligned} \quad (23)$$

III. PHASE DIAGRAM AND TRICRITICAL POINTS

In this section, let us study the transition temperature (or the phase diagram) and the tricritical points of the system. In the pure case with a finite transverse field the S_i^z component of the system is disordered at high temperatures, but below a transition temperature T_c it orders so that $m_z \neq 0$ and the direction of the moment changes continuously, although there is an order with $m_x \neq 0$ at all temperatures. In particular, for a strong random field, a tricritical point may be expected in the phase diagram for a bimodal distribution of $P(H_i)$.

Here we are interested in studying the transition temperature of the system. Expanding the right-hand side of Eq. (10) and Eq. (21), we obtain

$$m_z = A m_z + B m_z^3 + \cdots , \quad (24)$$

$$q_z = A' + B' m_z^2 + \cdots , \quad (25)$$

with

$$A = zp \sinh(J\nabla)[pq_z \cosh(J\nabla) + 1 - pq_z]^{z-1} \bar{F}(x)|_{x=0} , \quad (26)$$

$$B = \frac{z!}{3!(z-3)!} p^3 \sinh^3(J\nabla) \times [pq_z \cosh(J\nabla) + 1 - pq_z]^{z-3} \bar{F}(x)|_{x=0} , \quad (27)$$

and

$$A' = [pq_z \cosh(J\nabla) + 1 - pq_z]^z \bar{H}(x)|_{x=0} , \quad (28)$$

$$B' = \frac{z!}{2!(z-2)!} p^2 \sinh^2(J\nabla) \times [pq_z \cosh(J\nabla) + 1 - pq_z]^{z-2} \bar{H}(x)|_{x=0} . \quad (29)$$

By substituting Eq. (25) into Eq. (24), one obtains in general an equation for m_z of the form

$$m_z = a m_z + b m_z^3 + \cdots . \quad (30)$$

The second-order phase transition line is then determined by $a=1$, i.e.,

$$zp \sinh(J\nabla)[pq_z^0 \cosh(J\nabla) + 1 - pq_z^0]^{z-1} \bar{F}(x)|_{x=0} = 1 , \quad (31)$$

where q_z^0 is the solution of

$$q_z^0 = [pq_z^0 \cosh(J\nabla) + 1 - pq_z^0]^z \bar{H}(x)|_{x=0} . \quad (32)$$

In the vicinity of the second-order phase transition line, the magnetization m is given by

$$m_z^2=\frac{1-a}{b} . \tag{33}$$

The right-hand side of Eq. (33) must be positive. If this is not the case, the transition is of the first order, and hence the point at which $a=1$ and $b=0$ is the tricritical point.[51]

At this point, in order to obtain the expression for b, let us substitute

$$q_z=q_z^0+q_z^1m_z^2 \tag{34}$$

into Eq. (25). The expression of q_z^1 is then given by

$$q_z^1=\frac{f}{1-e} , \tag{35}$$

with

$$e=zp[\cosh(J\nabla)-1]\times[pq_z^0\cosh(J\nabla)+1-pq_z^0]^{z-1}\overline{H}(x)|_{x=0} , \tag{36}$$

$$f=\frac{z!}{2!(z-2)!}p^2\sinh^2(J\nabla)\times[pq_z^0\cosh(J\nabla)+1-pq_z^0]^{z-2}\overline{H}(x)|_{x=0} . \tag{37}$$

Substituting Eq. (34) into Eq. (24), the expression of b in Eq. (30) is given by

$$b=(z-1)zp^2q_z^1\sinh(J\nabla)[\cosh(J\nabla)-1]\times[pq_z^0\cosh(J\nabla)+1-pq_z^0]^{z-2}\overline{F}(x)|_{x=0}+\frac{z!}{3!(z-3)!}p^3\sinh^3(J\nabla)\times[pq_z^0\cosh(J\nabla)+1-pq_z^0]^{z-3}\overline{F}(x)|_{x=0} . \tag{38}$$

In previous work,[37,52] we have derived the phase diagrams of the spin-1 transverse Ising model with $H_i=0$ within the framework of the effective-field theory. There, the second-order critical lines ($a=1$ and $b<0$) in the T-Ω plane are analyzed for several lattice structures and compared with the mean-field predictions. The spin-1 phase boundary line for the honeycomb lattice is also compared with that of spin-$\frac{1}{2}$. The above expressions are general and are valid for a site-diluted transverse Ising model with a random field. In the following, three lattices, namely with $z=3$, $z=4$, and $z=6$ are investigated.

IV. NUMERICAL RESULTS AND DISCUSSION

A. Honeycomb lattices ($z=3$)

Putting $z=3$ into Eqs. (31) and (32) and Eqs. (36)–(38), we can get the phase diagrams of the system as functions of parameters T_c, p, Ω, and H.

Figure 1 shows the phase diagram in the T-Ω plane for the system with $H=1.0J$ for a given site dilution, namely, (a) 1.0, (b) 0.9, (c) 0.8, and (d) 0.75. With the decrease of p the phase region in which the ferromagnetic state is realizable gradually becomes small. As is seen from Fig.

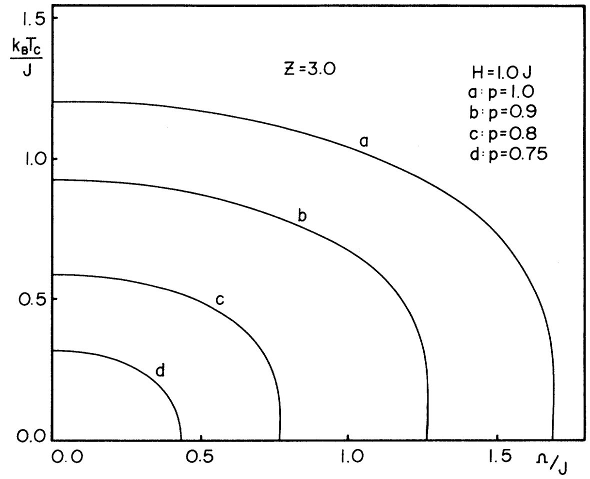

FIG. 1. Transverse field dependency of Curie temperature for the diluted spin-1 transverse Ising model with a random field, on honeycomb lattice ($z=3$), when $H=1.0J$ and p is changed.

1, on the other hand, when Ω increases from zero, in each curve T_c falls from its value at $\Omega=0$ and reaches zero at a critical value Ω_c.

Figure 2 shows the behavior of T_c as function of H for $\Omega=0$, when the value of p is changed, namely, (a) 1.0, (b) 0.8, (c) 0.7, and (d) 0.6. As is seen from the figure, in curves (c) and (d) T_c monotonically decreases and disappears at $H/J=1.0$. In contrast with them, the curves labeled (a) and (b) exhibit a bulge for the region of $H/J>1.0$, which results from the occurrence of reentrant phenomenon due to the competition between the fluctuations induced by the temperature, the exchange term, and the random field. Here, we should wonder if the reentrant phenomenon is an artifact due to our second approximation when taking the configurational averaging. However, the reentrant ferromagnetic (RF)

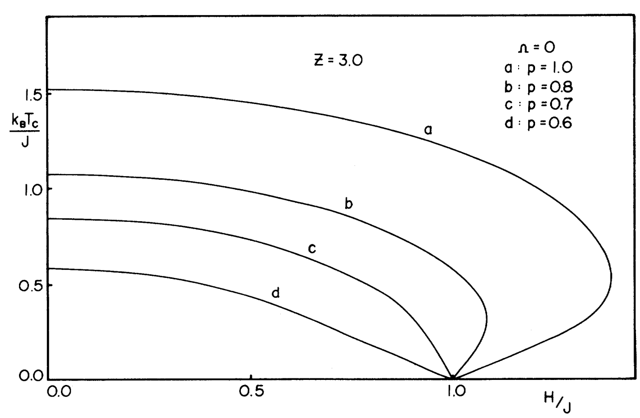

FIG. 2. Plots of T_c vs H for a diluted $S=1$ random-field Ising model ($\Omega=0$) with $z=3$, when p is changed as follows: (a) $p=1.0$; (b) $p=0.80$; (c) $p=0.70$; (d) $p=0.60$.

phase is a general characteristic of systems in which frustration and disorder are present.[60] There are higher and lower Curie temperatures in RF systems for which $E_u S_{r_{1-p}}$ S, is believed to an example.[61] Both, qualitative and quantitative accuracy of this question could be further increased by using other methods that provide a treatment beyond our effective-field framework. This is, however, a difficult task due to the complexity of the problem. The dilution plays some different role in the sense that the more diluted the system is, the more difficult it will be for some long-range order to be induced by the temperature fluctuations. By increasing the dilution the percolation of the clusters favoring the ferromagnetic order of the system becomes more difficult. In other words, these results indicate that the reentrant phenomenon observed in the pure system is suppressed when the dilution is performed.

Figure 3 shows the changes of T_c with p, for $\Omega=0$ with selected values of the random field, namely, (a) 0.0, (b) 0.80, (c) 1.05, (d) 1.10, and (e) 1.20. We investigate in detail the phase diagram in the region $0.0 \le H/J \le 1.20$, especially focusing on the situation with $H/J > 1.0$. Looking at Fig. 3, the critical lines exhibiting some characteristic behaviors; the first is that the bulge (or the reentrant phenomenon) gradually disappears with the increase of H. The second is that for the values of H smaller than unity, i.e., $0 < H/J < 1.0$, curve (a) presents the well-known behavior of the pure case. By increasing H, the T_c curve presents a downward curvature and goes to zero for a large value of p. On the other hand, this behavior is drastically changed when the value $H/J = 1.0$ is reached, critical value above which the competition effects are such that the reentrant phenomenon appears.

B. Square lattice ($z=4$)

For our diluted transverse Ising model with $z=4$, we can obtain the expression of the coefficients and the parameter q_z^0, as in Sec. III for $z=3$. Using these expressions, the behaviors of T_c as functions of Ω and H for

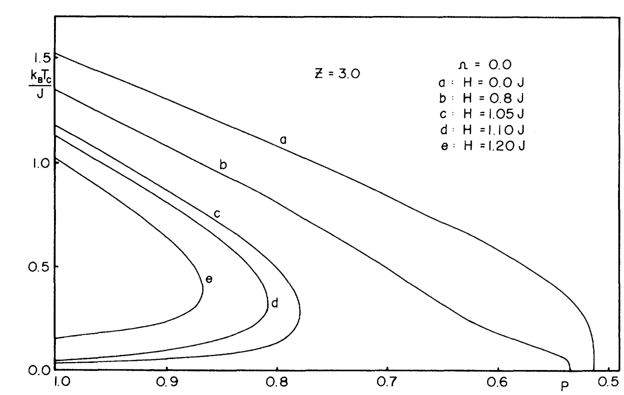

FIG. 3. Phase diagrams of the effective-field theory for the diluted spin-1 random field with $z=3$ when the value of H is changed as follows: (a) $H=0.0J$; (b) $H=0.80J$; (c) $H=1.05J$; (d) $H=1.10J$; (e) $H=1.20J$.

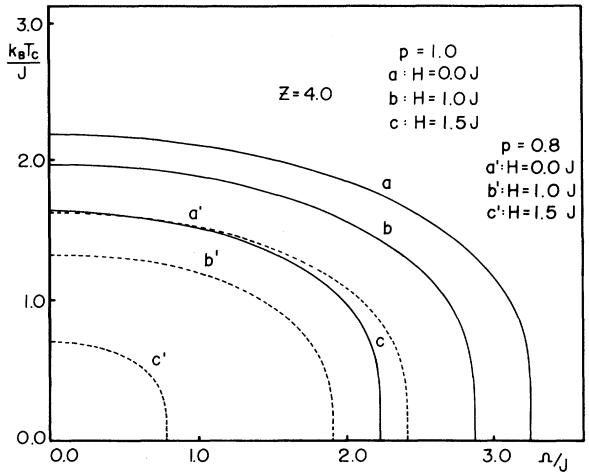

FIG. 4. Transverse field dependency of T_c for a diluted $S=1$ TIM with a random field on a square lattice ($z=4$). Solid ($p=1.0$) and dashed ($p=0.8$) lines are presented for selected values of H, namely, (a) $H=0.0J$, (b) $H=1.0J$, (c) $H=1.5J$.

selected values of p can be studied by solving Eqs. (32) and (33) with the help of (36)–(38).

Figure 4 shows the phase diagram in the T-Ω plane for the system with a fix p ($p=1.0$, full line and $p=0.8$, dashed line) for selected values of the random field, namely, (a) 0.0, (b) 1.0, and (c) 1.5, respectively. In order to discuss the tricritical behavior, the spin-$\frac{1}{2}$ random-field Ising model with a value of Ω (including $\Omega=0$), has been investigated by Sarmento and Kaneyoshi,[29] and there is shown that the system does not exhibit the tricritical behavior in the phase diagram, when the probability distribution function $P(H_i)$ is taken as a bimodal one and

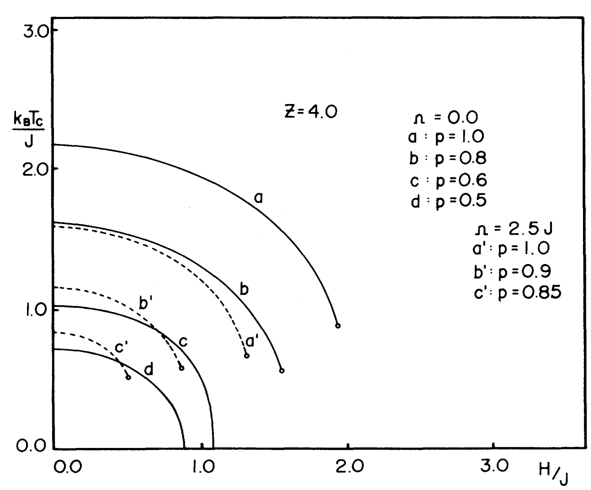

FIG. 5. Phase diagram in the T_c-H plane for $S=1$ random-field Ising model. Solid lines [$\Omega=0$ with (a) $p=1.0$, (b) $p=0.8$, (c) $p=0.6$, (d) $p=0.5$], and dashed lines [$\Omega=2.5J$ with (a') $p=1.0$, (b') $p=0.9$, (c') $p=0.85$] express the second-order transition lines. White circles denote the tricritical points.

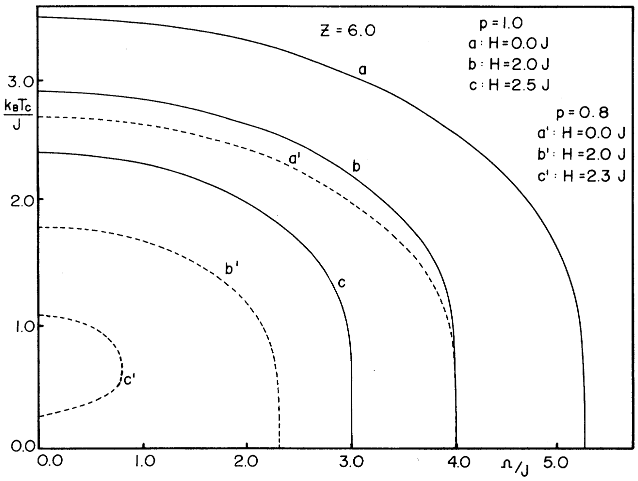

FIG. 6. Transverse field dependency of T_c for a $S=1$ TIM with a random field, on simple cubic lattice [$z=6$ when $p=1.0$ with (a) $H=0.0J$, (b) $H=2.0J$, (c) $H=2.5J$] solid lines, and $p=0.8$ [(a′) $H=0.0J$, (b′) $H=2.0J$, (c′) $H=2.3J$] dashed lines.

the coordination number is lower than $z=6$. Here, we find that the conclusion for spin-$\frac{1}{2}$ system is not valid for the spin-1 system. The second-order transition line and the tricritical point in the spin-1 random-field Ising model with a finite value of Ω on square lattice ($z=4$) can be evaluated when solving both the critical condition ($a=1$ and $b<0$), and the tricritical condition ($a=1$ and $b=0$) numerically.

Figure 5 shows the phase diagram in the T-H plane for the diluted spin-1 random-field Ising model with $z=4$. In the figure, solid ($\Omega=0$) and dashed ($\Omega=2.5J$) lines

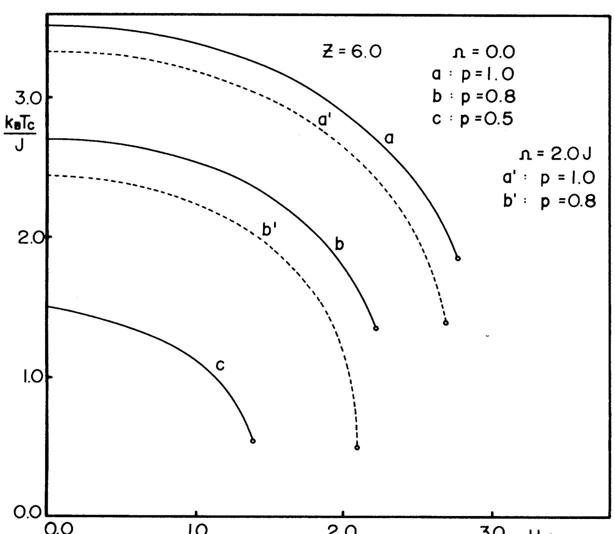

FIG. 7. Phase diagrams in the T_c-H plane for $S=1$ TIM with a random field, on simple cubic lattice ($z=6$). Solid lines [$\Omega=0$ with (a) $p=1.0$, (b) $p=0.8$, (c) $p=0.5$], and dashed lines [$\Omega=2.0J$ with (a′) $p=1.0$, (b′) $p=0.8$] denote the second-order transition lines. White circles express the tricritical points.

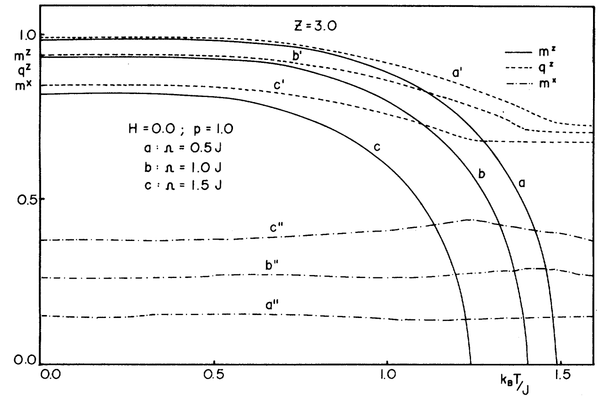

FIG. 8. Temperature dependency of sublattice magnetizations (m_z solid and m_x dotted lines), and the parameter q_z, for the pure TIM honeycomb lattice ($z=3$), when Ω is taken as (a) $\Omega=0.5J$, (b) $\Omega=1.0J$, (c) $\Omega=1.5J$.

denote the second-order transition, and white circles express the tricritical points. The tricritical temperature decreases monotonically with increasing Ω, and is very sensitive to the dilution changes.

C. Simple cubic ($z=6$)

In Fig. 6, the critical temperature is plotted as a function of Ω, for fixed values of p ($p=1.0$, full line and $p=0.8$, dashed line) and selected values of H, namely, (a) 0.0, (b) 2.0, and (c) 2.5. Figure 7 shows the phase diagram in the T-H plane ($z=6$) for $\Omega=0$ (full line) and $\Omega=2.0J$ (dashed line) and selected values of p. The white circles in the end of the second-order transition lines denote the tricritical points. The discussion here is similar to the square lattice case.

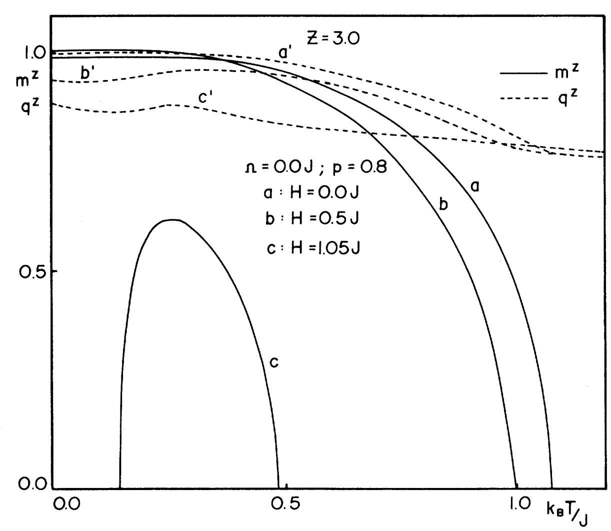

FIG. 9. Temperature dependency of m_z (solid), and q_z dashed lines at a fixed pair of values ($p=0.8$ and $\Omega=0.0$), for the diluted spin-1 with a random field on honeycomb lattice ($z=3$) and selected values of H: (a) $H=0.0J$; (b) $H=0.5J$; (c) $H=1.05J$.

V. MAGNETIZATION CURVES

The typical behavior of the longitudinal (full lines) and transverse (dotted lines) magnetizations, and quadrupolar moments (dashed lines) as function of temperature for $z=3$ is shown in Fig. 8 for $H=0.0$ and $p=1.0$ for selected values of Ω, namely, (a) 0.5, (b) 1.0, and (c) 1.5, respectively. Clearly the greater the transverse field, the smaller is the longitudinal magnetization. At $T=T_c$, m_z reduces to zero and q_z express the discontinuity for its derivative which is similar to that known for the spin-1 isotropic Ising model studied in Ref. 53. The role of the transverse field Ω is essentially to inhibit the ordering of m_z components; in the ordered phase m_x weakly depend on temperature.

In Fig. 9, the behavior of m_z and q_z as a function of T for a honeycomb lattice are shown for fixed pair values ($p=0.80$ and $\Omega=0.0J$) and several values of H, namely, (a) 0.0, (b) 0.5, and (c) 1.05. As is predicted in the phase diagram from Fig. 2, the reentrant phenomenon is observed in the magnetization curve of m_z, namely curve (c) with $H=1.05J$. By increasing H from this value, a critical field will be reached where the reentrant phenomenon will disappear with the ferromagnetic phase breakdown. Apart from slight variations due to the thermal agitation and competition effects, the discussion of the temperature dependence of q_z, which holds here, is similar to that of Fig. 8.

VI. CONCLUSIONS

In this work we have investigated the phase diagrams and magnetization curves of the diluted spin-1 transverse Ising model in a random field with a bimodal distribution on honeycomb, square, and cubic lattices by the use of an effective-field framework. The temperature (or transverse field) dependency of total longitudinal and transverse magnetizations for the system (with $z=3$) have been examined in Sec. V. In the present formulation the results depend only on the coordination number z but not on the dimensionality. However, the diluted Ising models normally simulate well the topologically disordered magnets, such as amorphous magnets, in which many physical quantities depend on the coordination number.[59]

The present effective-field approach is based on a further generalization of the Callen relation for the Ising model in the presence of a transverse field. The obtained results are quite remarkable considering that the approximation used within this simple effective-field approach neglects spin-spin correlations. Thus, as previous works on other models have indicated, we find that the results obtained herein can be given qualitative, and to a certain extent, quantitative liability.

We have shown that the phase diagrams include the tricritical point in the T-H plane below a critical transverse field, in contrast to the corresponding spin-$\frac{1}{2}$ counterpart. Thus, the tricritical behavior of the transverse Ising model in random field depends on the magnitude of spin. The behavior of tricritical point is also discussed as a function of Ω. The possibility of reentrant phenomena as discussed in Figs. 2, 3, and 9 has been predicted, which are due to the competition between the fluctuations induced by the temperature, the exchange term, and the random field. In Figs. 8 and 9 the magnetization curves are also determined as a function of the parameters p, Ω, and H.

ACKNOWLEDGMENT

This work was partially supported by CNPq (Brazilian agency).

---

*Permanent address: Universidade Federal de Alagoas, Departamento de Física, 57000, Maceió–AL, Brazil.

[1]P. G. de Gennes, Solid State Commun. **1**, 132 (1963).
[2]R. Blinc and B. Zeks, *Soft Modes in Ferroelectric and Antiferroelectrics* (North-Holland, Amsterdam, 1974); R. J. Elliott and A. P. Young, Ferroelectrics **7**, 23 (1974).
[3]R. J. Elliott, G. A. Gehring, A. P. Malogemoff, S. R. P. Smith, N. S. Staude, and R. N. Tyte, J. Phys. C **4**, L179 (1971).
[4]Y. L. Wong and B. Cooper, Phys. Rev. **172**, 539 (1968).
[5]R. Blinc and B. Zeks. Adv. Phys. Z **1**, 693 (1972).
[6]R. B. Stinchcombe, J. Phys. C **6**, 2459 (1973).
[7]S. Katsura, Phys. Rev. **127**, 1508 (1968).
[8]P. Pfeuty, Ann. Phys. (NY) **57**, 79 (1970).
[9]M. Suzuki, Phys. Lett. **34A**, 94 (1971).
[10]M. E. Fisher, J. Math. Phys. **4**, 124 (1963).
[11]R. J. Elliott and C. Wood, J. Phys. C **4**, 2359 (1971).
[12]P. Pfeuty and R. J. Elliott, J. Phys. C **4**, 2370 (1971).
[13]J. A. Plascak and S. R. Salinas, Phys. Status Solidi B **113**, 367 (1982).
[14]Y. Imry, J. Stat. Phys. **34**, 841 (1984).
[15]G. Grinstein, J. Appl. Phys. **55**, 2371 (1984).
[16]T. Nattermann and J. Villan, Phase Trans. **11**, 5 (1988).
[17]A. R. King, V. Jaccarino, D. P. Belanger, and S. M. Rezende, Phys. Rev. B **32**, 503 (1985).
[18]R. Bruinsma, *Nonlinearity in Condensed Matter,* edited by A. R. Bishop *et al.* (Springer, Berlin, 1987), p. 291 ff.
[19]S. Galam and J. L. Birman, Phys. Rev. B **28**, 5322 (1983); S. R. Salinas and W. F. Wreszinski, J. Stat. Phys. **41**, 29 (1985); T. Kaneyoshi, Physica **139A**, 455 (1985).
[20]O. Entin-Wohlman and C. Hartztein, J. Phys. A **18**, 315 (1985); M. Kaufman, P. E. Klunzinger, and A. Khurana, Phys. Rev. B **34**, 4766 (1986).
[21]H. E. Borges and P. R. Silva, Physica **144A**, 561 (1987); Phys. Status Solidi B **121**, K25 (1984).
[22]A. Aharony, Phys. Rev. B **18**, 3318 (1978).
[23]Y. Imry and S. K. Ma, Phys. Rev. Lett. **35**, 1399 (1975); M. Droz, A. Maritan, and A. L. Stella, Phys. Lett. **92A**, 287 (1982).
[24]P. Reed, J. Phys. C **18**, L615 (1985).
[25]D. P. Landau, H. H. Lee, and W. Kao, J. Appl. Phys. **49**, 1356 (1978).
[26]R. Honmura and T. Kaneyoshi, J. Phys. C **12**, 3979 (1979).
[27]V. K. Sakena, J. Phys. C **14**, L745 (1981).
[28]V. K. Sakena, Phys. Lett. **90A**, 71 (1982).
[29]E. F. Sarmento and T. Kaneyoshi, Phys. Rev. B **39**, 9555 (1989).

[30]T. Hai and Z. Y. Li, J. Magn. Magn. Mater. **80**, 173 (1989).
[31]M. Kaufman and M. Kanner, Phys. Rev. B **42**, 2378 (1990).
[32]A. Aharony, Y. Gefen, and Y. Shapir, J. Phys. C **15**, 673 (1982).
[33]T. Yokota and Y. Sugiyama, Phys. Rev. B **37**, 5657 (1988).
[34]F. S. Milman, P. R. Hauser, and W. Figueiredo, Phys. Rev. B **43**, 13 641 (1991).
[35]Y. Ma and Z. Li, Phys. Rev. B **41**, 11 392 (1990).
[36]Y. Ma, Z. Y. Li, D. L. Lin, and T. F. George, Phys. Rev. B **44**, 2373 (1991).
[37]I. P. Fittipaldi, E. F. Sarmento, and T. Kaneyoshi, Physica A **186**, 591 (1992).
[38]F. C. Sá Barreto, I. P. Fittipaldi, and B. Zeks, Ferroelectrics **39**, 1103 (1981).
[39]T. Kaneyoshi, E. F. Sarmento, and I. P. Fittipaldi, Phys. Rev. B **38**, 2649 (1988).
[40]T. Kaneyoshi, Physica A **175**, 355 (1991).
[41]M. Saber and J. W. Tucker, J. Magn. Magn. Mater. **114**, 11 (1992).
[42]H. B. Callen, Phys. Lett. **4**, 161 (1963).
[43]M. Suzuki, Phys. Lett. **19**, 267 (1965).
[44]E. F. Sarmento, R. B. Muniz, and S. B. Cavalcanti, Phys. Rev. B **36**, 529 (1987).
[45]E. F. Sarmento and T. Kaneyoshi, Phys. Status Solidi B **160**, 337 (1990).
[46]J. L. Zhong, J. L. Li, and C. Z. Yang, Phys. Status Solidi B **160**, 329 (1990).
[47]T. Kaneyoshi, E. F. Sarmento, and I. P. Fittipaldi, Phys. Status. Solidi B **150**, 261 (1988).
[48]T. Kaneyoshi, Physica A **164**, 730 (1990).
[49]G. B. Taggart and I. P. Fittipaldi, Phys. Rev. B **25**, 7026 (1982).
[50]I. P. Fittipaldi and T. Kaneyoshi, J. Phys. Condens. Matter **1**, 6513 (1989).
[51]N. Benayard, A. Benyoussef, and N. Boccara, J. Phys. C **18**, 1899 (1985).
[52]E. F. Sarmento, I. P. Fittipaldi, and T. Kaneyoshi, J. Magn. Magn. Mater. **104**, 233 (1992).
[53]T. Kaneyoshi, J. Phys. Soc. Jpn. **56**, 933 (1987).
[54]F. Zernike, Physica A **565**, (1940).
[55]See Fig. 5 in Chap. 6 of the book, T. Kaneyoshi, *Introduction to Surface Magnetism* (CRC, Boca Raton, 1991).
[56]M. Saber and J. W. Tucker, J. Magn. Magn. Mater. **102**, 287 (1991).
[57]V. Dobrosavljevic, S. H. Adachi, and R. M. Stratt, Phys. Rev. B **37**, 3703 (1988).
[58]A. Bobak and P. Macko, J. Magn. Magn. Mater. **109**, 172 (1992).
[59]T. Kaneyoshi, *Introduction to Amorphous Magnets* (World Scientific, Singapore, 1992).
[60]B. T. Cong, J. Magn. Magn. Mater. **117**, 126 (1992).
[61]P. J. Ford, Contemp. Phys. **23**, 141 (1982).